Cumhuriyet Science Journal

e-ISSN: 2587-246X
ISSN: 2587-2680

Cumhuriyet Sci. J., 42(4) (2021) 951-964
http://dx.doi.org/10.17776/csj.903575

Investigation of joining properties of AA 5083 material in MIG and TIG weldings

Hatice VAROL ÖZKAVAK [1,*] ***Serdar MERCAN*** [2]

[1] *Isparta University of Applied Science, Mechanical and Metal Tech. Dpt.,32200, Isparta, TURKEY*
[2] *Sivas Cumhuriyet University, Faculty of Technology, Mechatronics Eng. Dpt., 58140, Sivas, TURKEY*

Abstract

AA 5083 Aluminum alloys begin to be replaced steels in automobiles, ships, and high-speed-trains by providing reduced energy consumption and low carbon emissions thanks to their low densities, good weldabilities, and high corrosion resistance. During the production of high-speed trains, which are of special importance for our country, the proper selection of joining method for AA5083 increases the production speed. In this study, AA5083 alloys with 8 mm thickness were butt-welded under different parameters by using MIG and TIG weldings. It was aimed to determine the changes in microstructure and mechanical properties of welded samples, and also to specify the proper welding method. As a result, it was found that samples joined by MIG welding have higher strength and ductility, along with a lower amount of microstructural defects compared to their counterparts joined by TIG welding.

Article info

History:
Received: 26.03.2021
Accepted: 05.10.2021

Keywords:
TIG,
MIG,
AA5083,
Mechanical properties,
Microstructure.

1. Introduction

Aluminum, also known as green material, is the 3rd most commonly found element on Earth [1-3]. Al, the most common material used as an alternative to steel for many applications in design and production, has many important properties as low weight, excellent impact resistance, ideal corrosion resistance, and recyclability [4,5]. For this reason, Al and its alloys have found widespread use in many sectors such as the automotive, railway, aerospace, and shipbuilding industries [6]. 5XXX Al series are widely used for structures in shipbuilding. These alloys have a high strength/weight ratio, good weldability, and excellent corrosion resistance against sea conditions [7,8]. The strength of AA5083 alloy, which contains 4.5% Mg and %1 Mn in its chemical composition, can be increased by strain-hardening or solid solution strengthening in concentrated Mg [9]. In many industrial applications where Al alloy is used, there are complex structures that require highly efficient nondetachable connections. It is determined that, under static and dynamic loadings, welded Al alloys in such complex structures show more efficiency compared to rivet joints [10]. Besides, the use of welded joints in the joining of Al alloys reduces the cost by 60-65%. Metal Inert Gas (MIG) and Tungsten Inert Gas (TIG) welding methods are widely used in joining Al alloys [11]. When arc-welding methods are used for Al alloys, fatigue damage, brittle fracture, and stress-corrosion cracks occur due to distortion and residual stress [12]. To reduce residual stresses and prevent distortion, pre-/intra-welding [15,16] or post-welding [17,18] mechanical and thermal processes [13,14] were discussed in many studies. In TIG welding, which is widely used for joining Al and its alloys, an electric arc is created between the non-consumable tungsten electrode and the workpiece. In this method, an electrode holder is used to fix the non-consumable tungsten electrode. When electrical power is applied between the electrode and the workpiece, the gas passes through the cylinder and reaches the nozzle around the electrode. The gas surrounds the arc, protecting the welding area from atmospheric effects and preventing defects [19]. On the other hand, MIG welding is performed by feeding a continuous solid wire electrode from a welding gun and weld pool. In both methods, protective gas is sent to the welding gun [20]. MIG welding method is more superior compared to TIG welding in terms of microstructure change, bonding capability, and welding metal deposition ability [21].

In their study, Yang et al. analyzed the electrochemical properties of Al 6082 joined by MIG and friction stir welding and stated that the corrosion rate of FSW

*Corresponding author. e-*mail address: haticevarol@isparta.edu.tr.*
http://dergipark.gov.tr/csj ©2021 Faculty of Science, Sivas Cumhuriyet University

joints was lower than the MIG joints [22]. Schneider et al. aimed to optimize the effects of TIG-MIG/MAG hybrid welding techniques on welding geometry. At the end of the study, the most effective parameters were found as the type of protective gas (MIG-MAG), voltage (MIG-MAG), wire feed speed (MIG-MAG), along with welding speed and density of the electric current (TIG) [23]. Subbaiah investigated the microstructure and mechanical properties of casted Al-Mg-Sc alloy after TIG welding. It was stated that the TIG-welded Al-Mg-Sc alloy casting has improved tensile properties compared to the main material. Furthermore, the author confirmed a decrease in strength due to Mg vaporization [24]. In their study, Zhang et al. compared the joining properties of laser and TIG welding methods for AlSi10Mg samples manufactured by SLM and casting techniques. Welding morphology, defects, microstructure, and mechanical properties were discussed in the study. As the result of the study, it was concluded that the gaps present within SLM samples causes defects during welding, laser shows better welding properties and higher tensile strength than TIG welding for SLM parts. It was also stated that tensile strength of SLM-SLM or SLM-casting joining is superior in comparison with the main material [25]. Shu-Fen studied the effect of welding current on morphology and microstructure of T joints for Al alloys joined by double-pulse MIG welding. The authors stated that the width and depth of the welding seam increase by rising the average current, and the most optimal properties are achieved at a current of 90 A. Singh et al. deduced that tensile strength shows a significant increment by increasing welding current and gas flow rate [26]. In addition to this, Kumar et al. investigated the effect of heat input on the strength of the joining area and found that the tensile strength decreases with heat input increment [27]. Similarly, Jahanzaib et al. concluded that if a high welding current and low welding speed are selected, the quality of the welded connection improves [28]. Raveendra et al. examined the effect of the welding current on the weld seam and obtained a linear increase in the front and back side by increasing the welding current [29]. Gharibshahiyon et al. stated that high heat input causes grain growth along with toughness and impact energy reduction in welded joints [30].

Mg is the main element of 5000 series Al alloys. Thanks to their low densities, good weldabilities, and high corrosion resistance, AA5083 Aluminum alloys begin to be replaced steels in automobiles, ships, and high-speed-trains by providing reduced energy consumption and low carbon emissions [31]. Thus, the joining process of Al alloys plays an important role. In the literature, there are studies on the joining of AA5083 Al alloys. By investigating mechanical properties and microstructure of AA5083 alloy by FSW method, it is seen that reduction in friction heat input leads to high ductility, good formability, and betterment in grain size [32]. In other studies, two different porosity structures that occurred during the laser welding of AA5083 Al alloys were examined, and it was concluded that the number of porosities can be reduced in case of using a double beam source as welding [33,34].

In this study, AA5083 alloys with 8 mm thickness were joined under different parameters by using MIG and TIG weldings. In this study, the gap in the literature has been tried to be closed by considering the values that are not used in the literature in terms of both the thickness of the joined part and the process parameters used.The mechanical properties and microstructure of the welded joints were analyzed.

2. Materials and Methods

In this study, AA5083 Aluminum plates were joined via MIG and TIG weldings. In the experiments, plates with 8 mm thickness were used. Samples were procured from GÖK YAPI AŞ and joined in TÜDEMSAŞ Welding School. After welding, the samples were cooled to room temperature. The chemical composition of the AA5083 alloy selected for this study is given in Table 1, and mechanical properties are given in Table 2.

Table 1. Chemical composition of AA5083 Aluminium alloy

Fe	Si	Cu	Mn	Mg	Zn	Cr	Ti	Other	Al
0,40	0,40	0,10	0,40-1,0	4,0-4,9	0,25	0,05-0,25	0,15	0,15	Balance

Table 2. Mechanical properties of AA5083 Aluminium alloy

Density (gr/cm^3)	Brinell Hardness (HB)	Tensile Strength (MPa)	Yield Strength (MPa)	Elasticity Module (GPa)
2,66	85	317	228	71GPa

The main objective of the study is to determine the optimum welding method by examining the change in microstructure and mechanical properties of AA5083 alloy joined with TIG and MIG methods under different process parameters. The workflow of the study is given in Figure 1.

Welding parameters used in the experiments are given in Table 3. While selecting the welding parameters, the process parameters used in previous studies were evaluated, and originality was ensured in the study by choosing different parameters from these parameters [1,35,38]. Zirconiated Tungsten (98%W+2%Zr) electrode is used with 2,4mm diamaeter for TIG welding proceses. 1,6 mm wire diameter is used for MIG welding process.

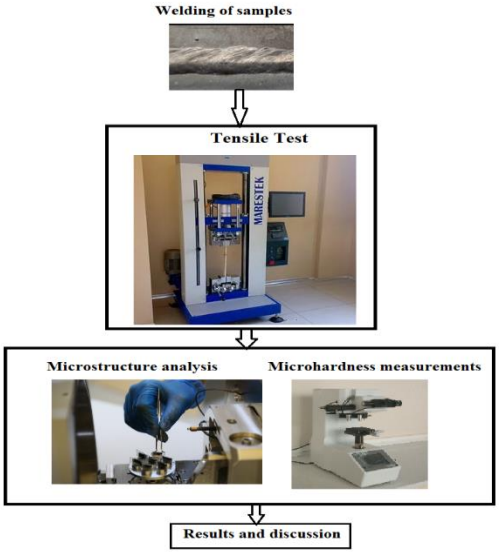

Figure 1. Workflow of the study

Table 3. Welding parameters used in the study

Method	Sample Number	Current (A)	Voltage (V)	Speed (mm/s)	Torch Distance (mm)
MIG	S1	150	18	2,6	15
	S2	170	20	2,7	
	S3	180	22	2,3	
	S4	190	23	2,5	
Method	**Sample Number**	**Current (A)**	**Tungsten electrode diameter (mm)**	**Speed (mm/s)**	**Stand-off distance (mm)**
TIG	S5	140	2,5	2,4	5
	S6	160		3,1	
	S7	180		4	
	S8	200		5	

Plate samples joined with different process parameters are given in Figure 2. After the joining process, the samples were prepared for microstructure analysis, microhardness measurement. During the preparation of the samples, the cutting operations were performed in the Electrical discharge machining (EDM) device to prevent the samples from being exposed to any hot or cold deformation. For microstructure analysis of welded samples in the study, test pieces were cut from the cross-section of the weld. Subsequently, the test pieces were sanded by 400,800,1500 grit sandpapers and polished with broadcloth, respectively. Finally, surface polished test pieces were etched in Keller solution (2 ml HF, 3 ml HCl, 5 ml HNO3, and 190 ml H2O) and prepared for microstructure analysis. In addition, SEM examinations were performed on the FEI QUANTA FEG 250 device to determine the grain structure and porosity within the weld area.

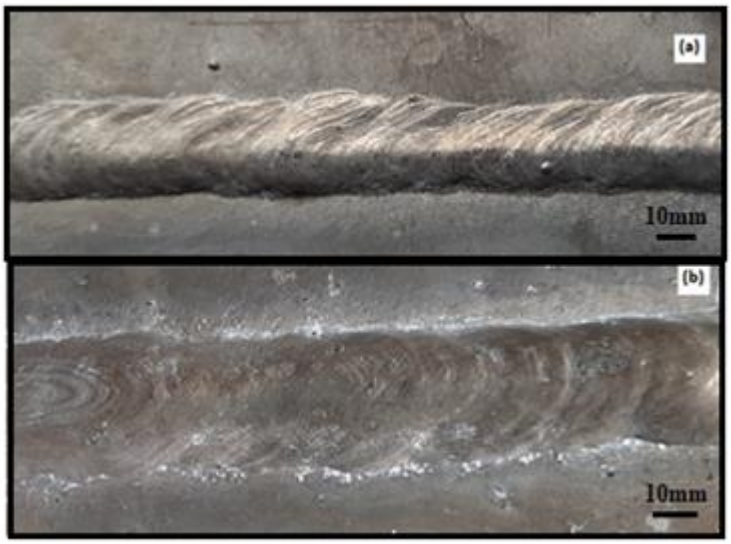

Figure 2. Images of plate samples joined by (a) MIG welding (b) TIG welding

To determine the weld area strength of welded samples, a Marestek brand tensile test device was used. The samples used in the tensile test were prepared in accordance with ASTM EN ISO 4136 standards. Analysis of the sample regions is given in Figure 3. Tensile tests were carried out at room temperature with a speed of 0.5 mm.

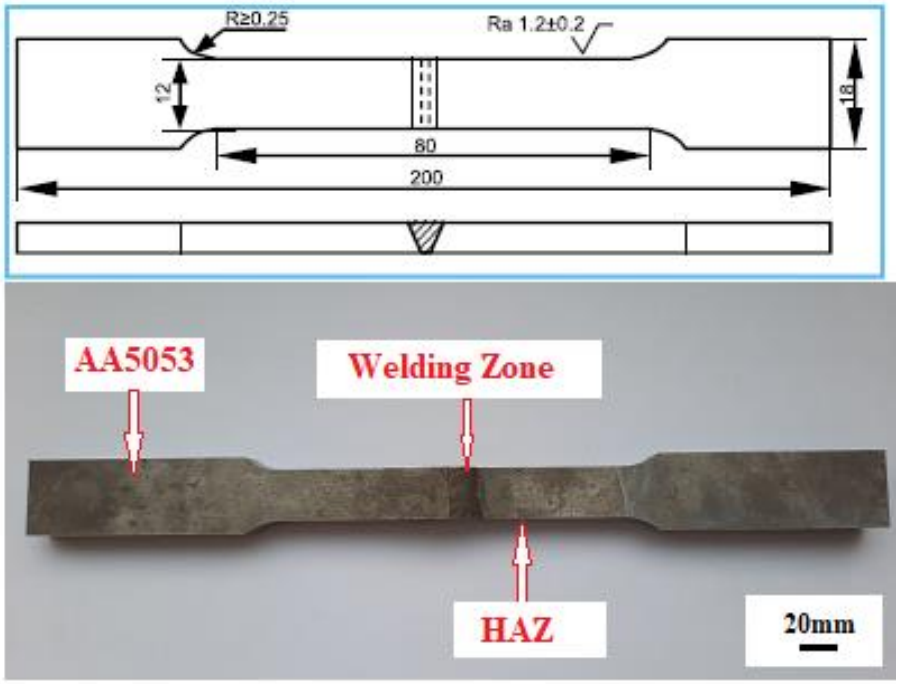

Figure 3. Tensile test specimens used in the study

Vickers microhardness measurement was carried out at 300g load to determine the change in hardness after the joining process. Microhardness measurements were taken from three different points: the heat-affected zone (HAZ), the base material (MB), and the weld zone (WZ). The measurements points are shown in Figure 4. The measuring range is set at 0.5 mm.

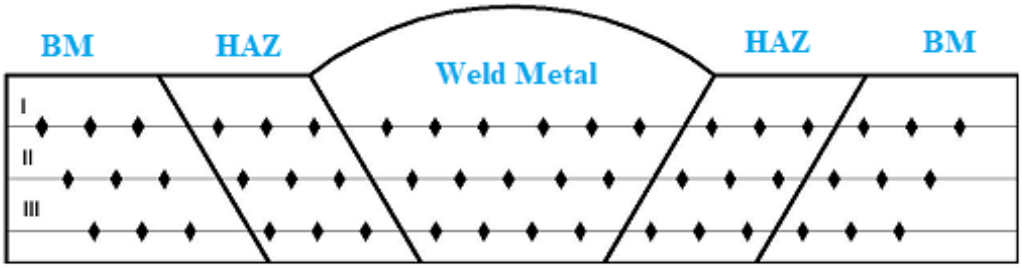

Figure 4. Microhardness measurement points

3. Results and Discussion

3.1. Macro and microstructure analyzes

In the study, 8 mm thick AA5083 alloys were joined by TIG and MIG welding methods using different welding parameters. Macrostructure images of the welded samples are given in Figure 5. In Figure 5, it is seen that defects such as pore and spatter were encountered in samples joined by the TIG welding method. It is thought that incomplete melting causes these specific defects within the welding zone [1]. When the MIG-welded samples are examined, it is clearly observed that the weld root is smoother since the melting is accurately accomplished. This situation can be explained by the fact that the joining is performed perfectly in the MIG welding method. When this situation seen in the macrostructure analysis is evaluated together with the tensile test results, the results overlap with each other.

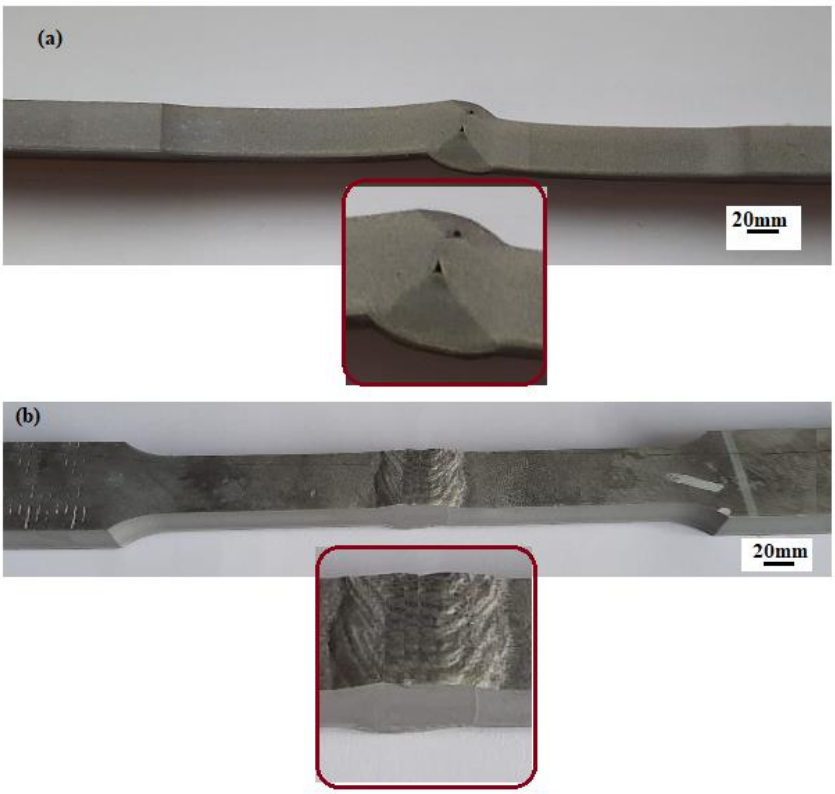

Figure 5. Macro images of welded samples (a) TIG welding (b) MIG welding

The post-tensile test macro structure images of the samples joined by TIG and MIG welding methods are given in Figure 6. When Figure 6 is examined, it is observed that the fracture starts from the porosity region in the TIG welded samples. This situation can be explained as an indication of the low mechanical

properties of the samples joined by the TIG welding method. In Figure 7, macro images of all tensile samples are given. When Figure 7 examined the fractures had occurred in the weld metals for the samples joined with a lower welding current. This was because a lower welding current leads to poor penetration on the joints [1].

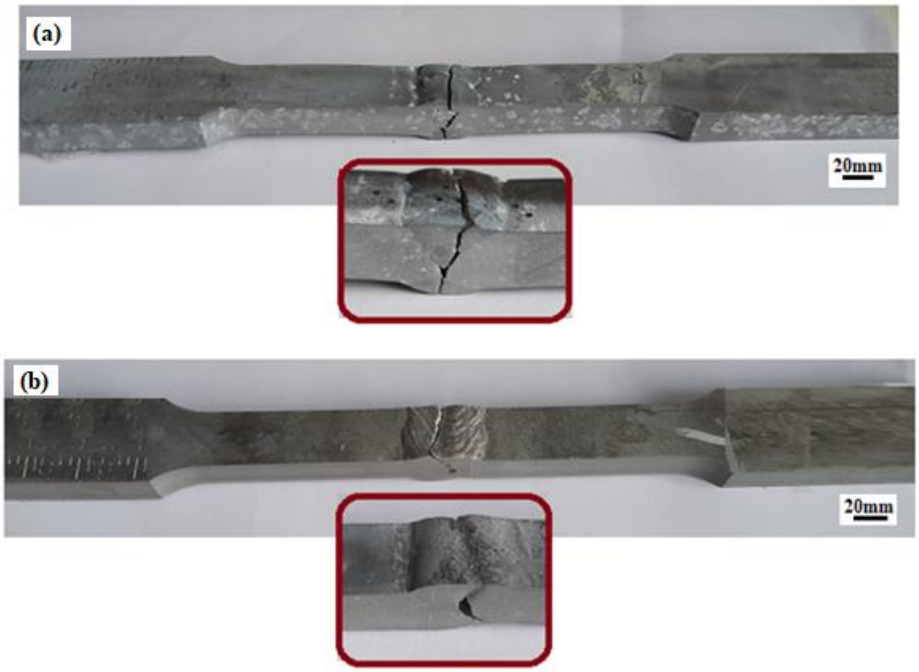

Figure 6. Macro images of welded samples (a) TIG welding (b) MIG welding

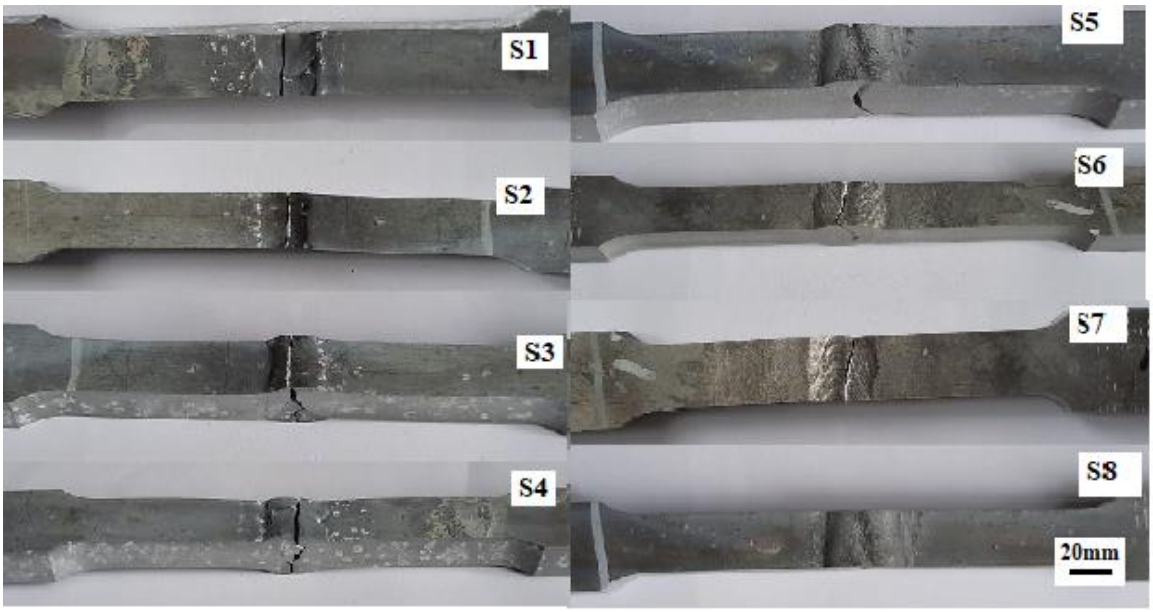

Figure 7. Macro images of tensile samples

In addition to the macrostructural analysis of welded samples, their microstructural analysis was carried out as well. Microstructural analyses were performed in base metal and weld zone areas, as given in Figure 8. Different weld zone width for each sample was taken into account during the conduction of experiments.

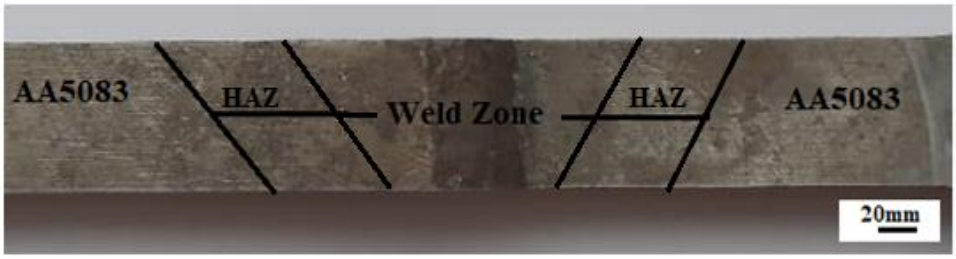

Figure 8. Microstructure analysis areas for the samples

In Figure 9, microstructure images of the welded zone for the MIG welded samples are given. At the S4 sample in Figure 9 (S4), which is processed with the highest welding current, a growth in grain size can be seen. This situation can be explained as the elevation in heat input due to the increasing current. A similar case can be seen for the S3 sample as well. In the S1 sample, for which the welding current was selected as 150 A, and the S2 sample, where the welding current was 170 A, the heat input did not cause grain coarsening, on the contrary, it provided a better grain formation. When Figure 9 is examined, it is possible to talk about a typical one-directional solidified microstructure. Whether this solidified grain structure obtained in the MIG method is columnar or coaxial depends on the solidification rate [36]. Rapid solidification occurs in the MIG method. Fine grain size is formed as a result of rapid solidification in the MIG method. It is also seen that spherical-shaped porosities are found within the samples joined by MIG welding. The formation of these porosities is due to the hydrogen solubility in molten aluminum.

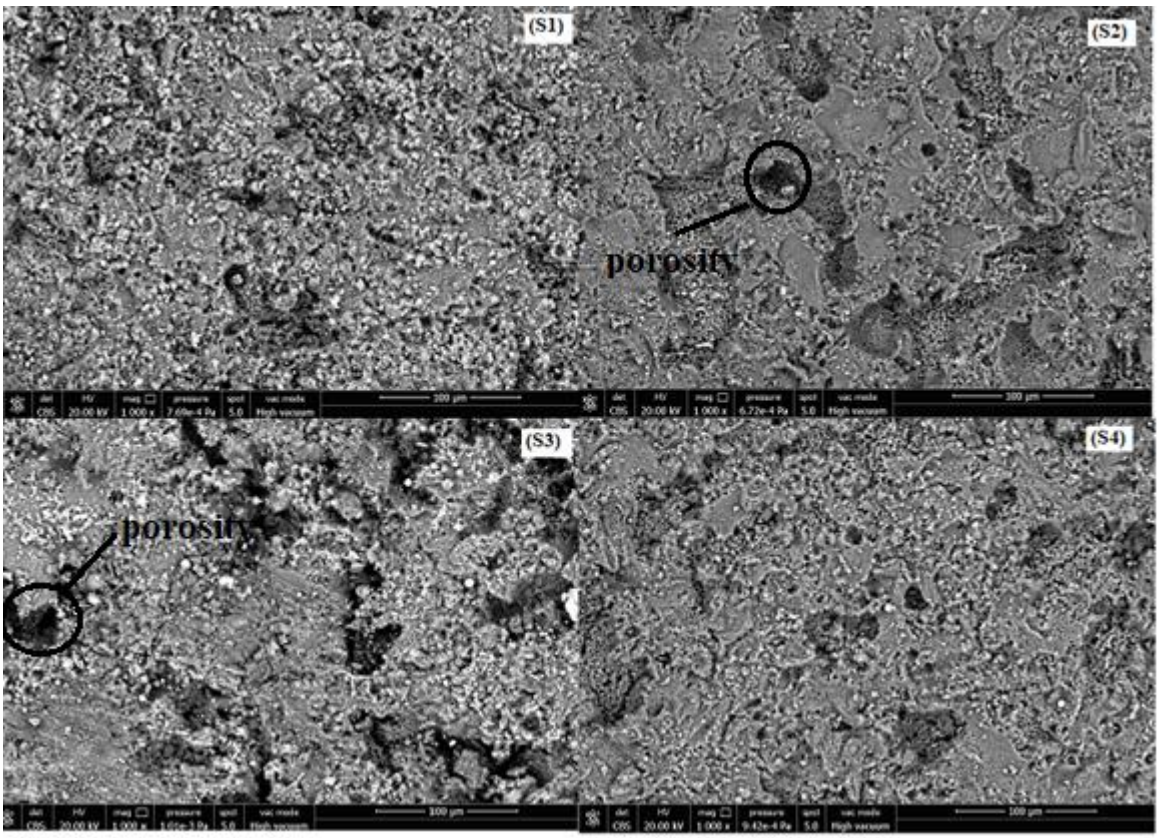

Figure 9. Microstructure images of welding zones of MIG welded samples

Figure 10 shows the microstructure images of the weld area of the samples joined by TIG welding. When TIG-welded samples are examined, it is seen that despite the increment in the welding current decreases the grain growth, the grain size obtained in TIG welding has not reached the size obtained in MIG welding. This is

because the melt convection in TIG welding is slower than in MIG welding [37,38]. The gradient convection of the melting slows down the solidification and causes the grains to grow. With the increase of welding current, solidification moderately accelerates, which eventually decreases the grain size. For this reason, the largest grain size was obtained in the S6 sample where the welding current is 140 A. The temperature gradient difference in the TIG welding is different compared to MIG welding, which affects recrystallization. The amount of porosity formed in the samples joined by TIG welding is higher than the MIG welding method. The porosities within the samples were formed as a result of inhomogeneous heating and cooling processes.

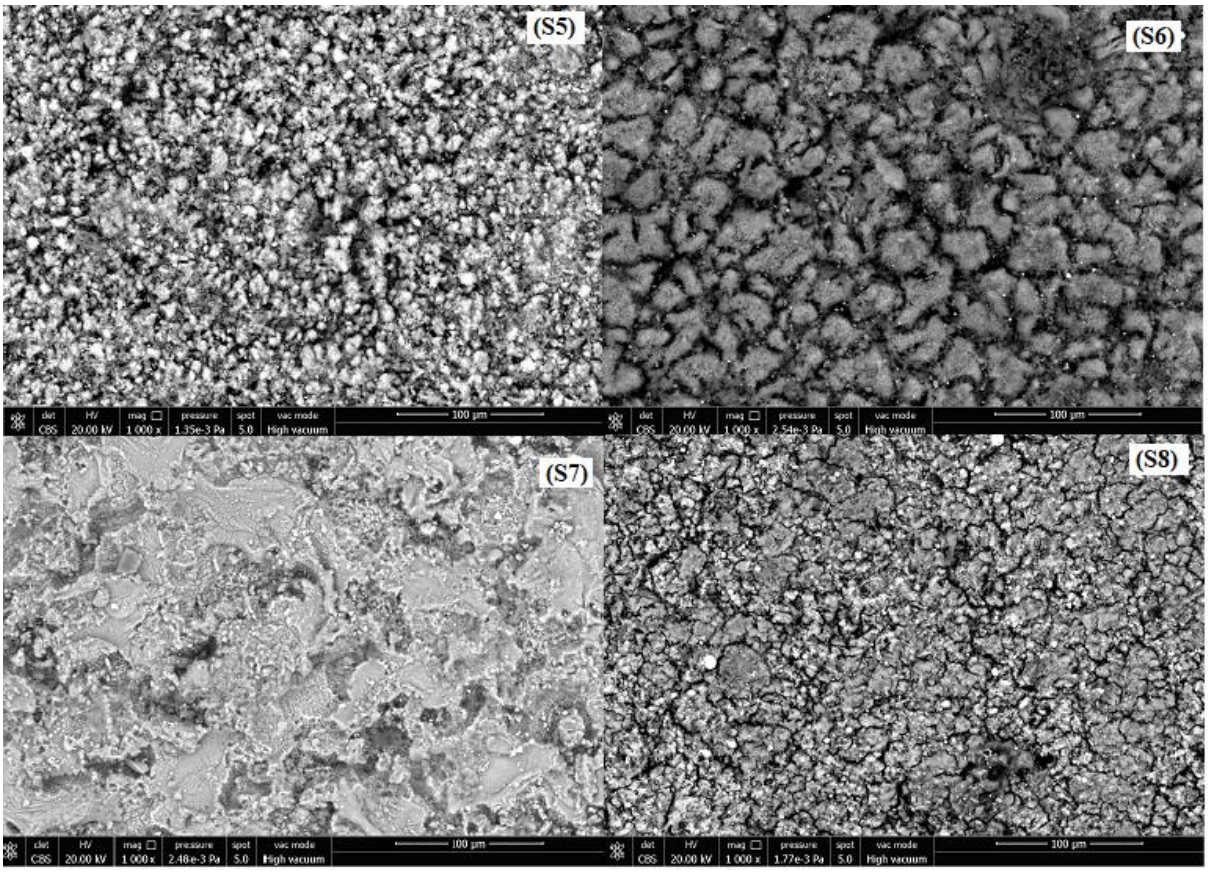

Figure 10. Microstructure images of welding zones of TIG welded samples

As a result of microstructure analyzes, it has been determined that the grain structure in MIG welding is favorable to TIG welding. Besides, it has been also observed that the second phase particles formed within the samples affect the strength and ductility [31].

3.2. Micro-Hardness tests

Microhardness measurements were made on samples joined with TIG and MIG weldings. Hardness values of TIG-welded samples are given in Figure 11, and hardness values of MIG-welded samples are given in Figure 12. By examining the hardness values of MIG-welded samples, it is seen that the average hardness value of the base metal is HV79±2, while the average hardness value of the weld zone is HV63±3. It is also observed that there is a decrease in hardness from the base metal towards the weld zone [44]. Therefore, the hardness value in the weld zone is 18% lower than the hardness value of the base metal in MIG welding. Along with it, hardness values in the HAZ region are higher than in the weld zone for MIG welded samples (Figure 12). This causes the hardness of the weld metal area to drop, as β-phase deposits occur during the welding process [7]. The β-phase (Figure- dark areas) occurring in the weld zone is due to the distribution of the solute in the structure during solidification and occurs with the formation of a solute-rich local region.

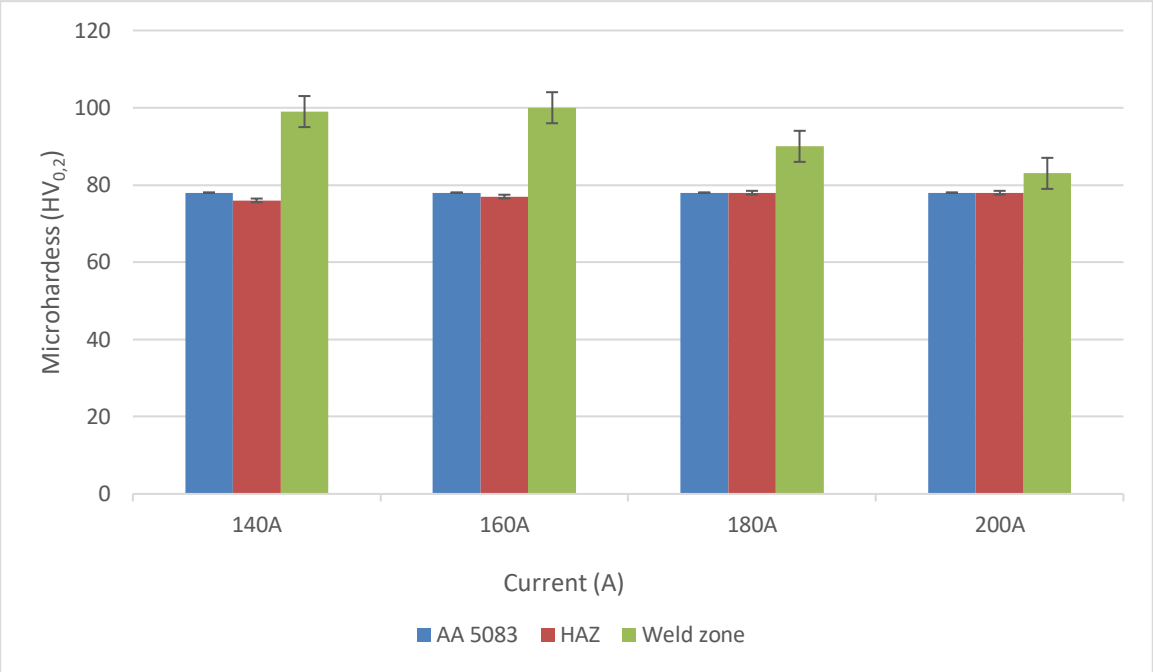

Figure 11. Microhardness values of TIG-welded samples

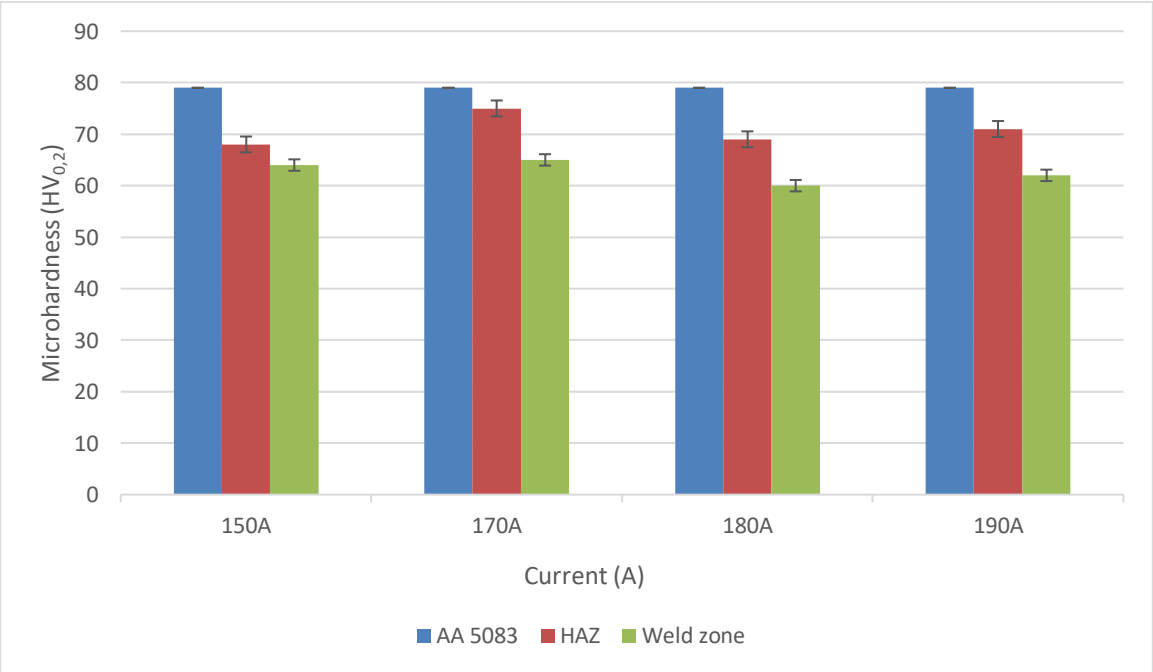

Figure 12. Microhardness values of MIG-welded samples

By examining the hardness values of TIG-welded samples, it appears that the average hardness value of the base metal is HV78±2, while the average hardness value of the weld zone is HV93±4. The hardness values of the HAZ region and the base material were achieved close to each other for the TIG-welded samples. However, the hardness values of the weld zone are higher than the other regions. This situation adversely affects the strength of the joining. With the increase in welding current, the hardness value of the weld zone decreases. This reduction in hardness leads to a betterment in the strength of the joints. Obtaining the hardness value higher even than the base metal can be explained as an indicator that the weld zone is brittle and fragile. When the macro and microstructures of the fractured surface of the TIG-welded samples are inspected, the brittleness of the fracture type in the weld zone confirms this result.

When the hardness distribution of MIG welding was examined, it was determined that the hardness value of the base metal was the highest. This can be explained as the heat input occurring during the welding process affects the main material properties (grain structure, grain size). In TIG welding, the hardness value of the weld zone was higher than the other zones. This is due to the fact that these regions have become more brittle structures.

3.3. Tensile tests

Tensile tests were applied to the samples in order to determine the mechanical properties after welding. The change in the tensile stress of the TIG-welded samples according to the welding current is given in Figure 13. The tensile test results of the samples combined with AA 5083, 140 A, 160 A, 180 A and 200 A welding currents are 317 MPa, 122 MPa, 105 MPa, 119 MPa and 125 MPa respectively. As Figure 13 indicates, the maximum tensile stress (125 MPa) could be obtained at 200 A. All welded samples were fractured from the weld zone during the tensile tests. This proves that the strength of the weld zone is less than the strength of the base material. Although the weld zone strength increases with the welding current increment, it could never reach the strength of the base material. Porosities formed within the weld zone and microstructural changes that occur during the solidification of the weld pool reduce the strength of the welded parts. In the study, porosities were clearly observed in the TIG-welded samples. Previous studies in literature verify this phenomenon [40-42]. In addition, the strength of the welded joint depends on the penetration depth as well. Welding current increase leads to deeper penetration, therefore the welded joint strengthens with the increasing welding current. Besides, since the root of the weld is partially joined, it acts as a stress formation zone, causing crack initiation and propagation, thus causes the joining strength to weakens [31]. One of the most considerable problems seen in TIG welding is grain coarsening that appears after slow solidification at the interfaces. The grain coarsening formation in the welded area significantly reduces the strength of this specific region.

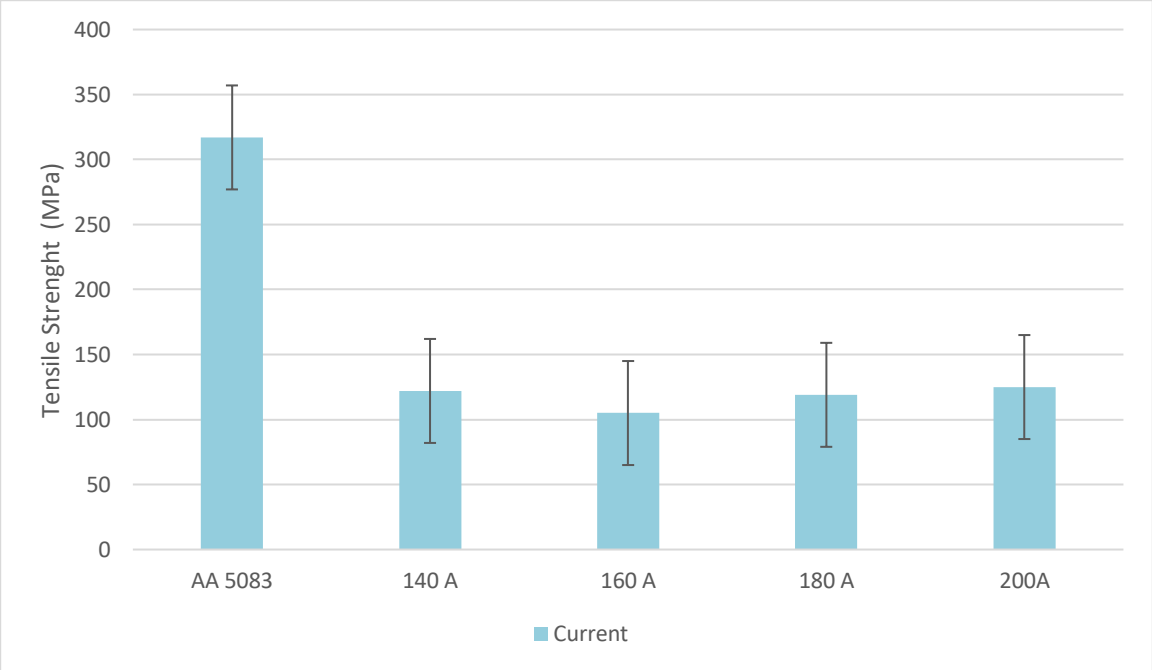

Figure 13. Tensile test results of TIG-welded samples

In this study, tensile tests for AA5083 alloys with 8 mm thickness were carried out to determine the mechanical properties after MIG welding at 150A, 170A, 180A, and 190A. The tensile test results of the samples combined with 150 A, 170 A, 180 A and 190 A welding currents are 301MPa, 305MPa,270 MPa and 263MPa, respectively, and are given in Figure 14. As the figure indicates, the maximum tensile stress (305 MPa) was obtained at 170 A. In operations where the welding current passes 170 A, the strength of the welded joints decreases again. With the increase of the welding current value, the temperature of the welding zone elevates; thus causes the microstructure of the joint area to deteriorate and its strength to decrease. The grain structure solidified in the weld zone changes depending on the cooling rate. Since cooling is faster

in MIG than TIG, a dendritic internal structure was formed. With the increase of the current in MIG welding the temperature gradient difference, which significantly affects the recrystallization process, leads to a decrease in work-hardening and eventually causes a decrease in strength [43]. Furthermore, it causes coarse-graining due to welding current increment, which also leads to a reduction in strength. For this reason, with the increase of the welding current in MIG welding, a decrease in the strength for welded samples takes place again. The strength values obtained in the process of joining with MIG welding are very close to the yield stress value of the main material (317 MPa). This clearly shows that 170A is the most suitable parameter for MIG welding.

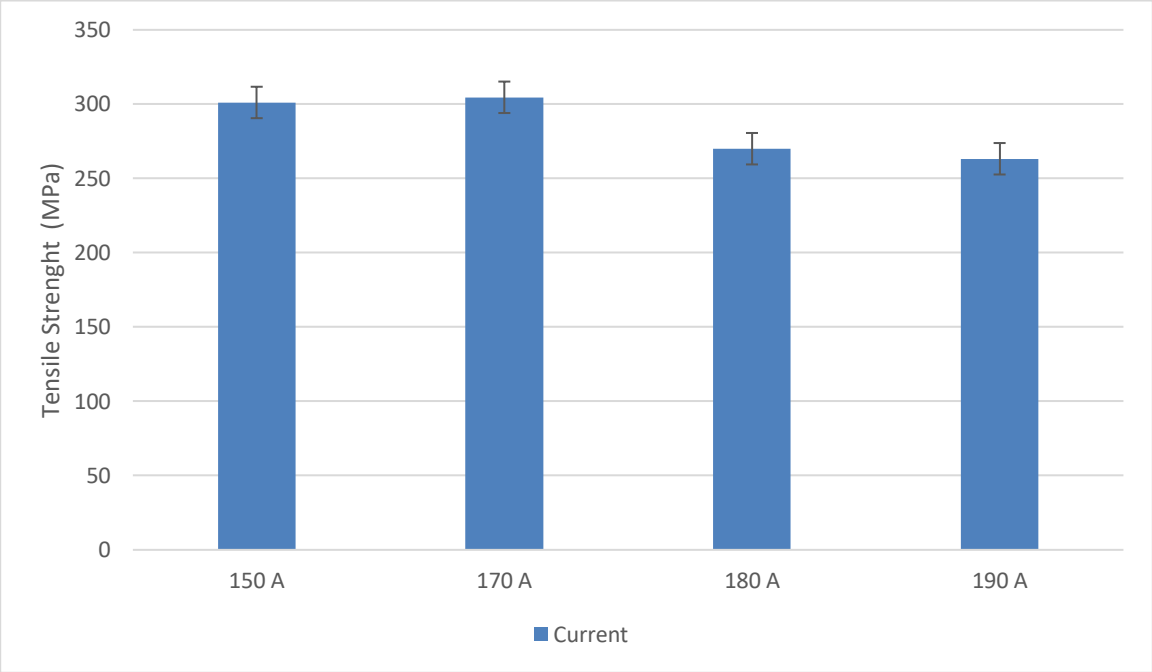

Figure 14. Tensile test results of MIG-welded samples

In the study, microstructure analyzes of the broken surfaces after the tensile test were also made. Broken surface evaluation for S4 and S6 samples, which are the samples with lowest strength values for both welding methods, was taken into consideration. In Figure 15, their microstructure examinations for both TIG ad MIG welding methods are given. Concentric grains exhibiting semi-ductile behavior in the base metal were observed during the AA 5083 core metal internal structure inspections. Dimples formed within the S4 sample are smaller than the ones in the parent material. Furthermore, sample S6 exhibited a fragile behavior. In either method, the main material is more ductile.

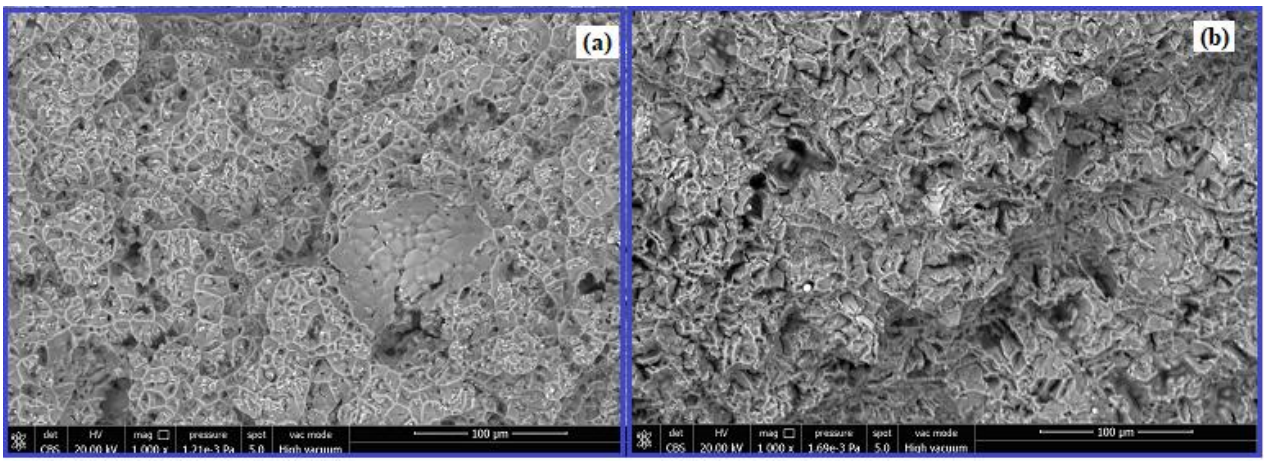

Figure 15. Post-tensile test macro structure images of broken surfaces (a) MIG-welded samples (b) TIG-welded samples

The tensile strength of the samples combined with the TIG method was lower than the samples combined with the MIG method. This is due to the formation of grain coarsening due to slow solidification during the welding process. In the TIG method, porosities occurred in the welding zone and this caused a decrease in strength. If the welding current selected for the MIG method exceeds 170 A, a decrease in strength is obtained; In the TIG method, the strength increases as the current increases.

4. Conclusion

In this study, AA5083 alloys with 8 mm thickness were butt-welded under different current values by using MIG and TIG weldings. The results are as follows:

The slow solidification occurring at the interfaces during the joining process with the TIG welding method leads to a grain growth, which caused the strength values to be lower than the MIG welding method.

The weld zone hardness values of the MIG welding were obtained lower than the TIG welding. On the other hand, the hardness value of the weld zone was higher than the base metal in the TIG welding method. These high hardness values are an indication that the welding zone is brittle and fragile.

Maximum tensile stress of 125 MPa for TIG-welded sampes was acquired at 200 A. It is also concluded that more current value in TIG welding means higher strength.

For MIG-welded samples, maximum tensile stress of 305 MPa was acquired at 170 A. A decrease in tensile strength was seen when the current value exceeded 170 A. For this reason, the most suitable current value for MIG welding method was determined as 170 A.

Acknowledgment

We would like to thank GÖK YAPI AŞ and TÜDEMSAŞ Welding Training and Technology Center.

Conflicts of interest

The authors state that did not have conflict of interests

References

[1] Mercan E., Ayan Y., Kahraman N., Investigation on joint properties of AA5754 and AA6013 dissimilar aluminum alloys welded using automatic GMAW, *Engineering Science and Technology, an International Journal,* 23 (2020) 723-731.

[2] Franz D., Szilvasi T., Irran E., Inoue S., A monotopic aluminum telluride with an Al= Te double bond stabilized by N-heterocyclic carbenes, *Nature Communication,* 6 (2015) 1-6.

[3] Zamzami I.A., Susmel L., Nominal and local stress quantities to design aluminium-to-steel thin welded joints against fatigue, *International Journal of Fatigue,* 101 (2) (2017) 137–158.

[4] Heinen P., Wu H., Olowinsky A., GillnerA., Helium-tight laser beam welding of aluminum with brillant laser beam radiation, *Physics Procedia,* 56 (2014) 554–565.

[5] Li J., Xue J., Zhang Z., Hu Y., Effects of thermal frequency on microstructures, *Applied Science,* 8 (4) (2018) 540.

[6] Borrego L.P., J.D. Costa, J.S., Jesus, A.R. Loureiro, J.M. Ferreira., Fatigue life improvement by friction stir processing of 5083 aluminium alloy MIG butt welds, *Theoretical and Applied Fracture Mechanics,*70 (2014)68-74.

[7] Ilman M.N., Triwibowo N.A., Wahyudianto A., Muslih M.R., Environmentally assisted fatigue behaviour of stress relieved metal inert gas (MIG) AA5083 welds in 3.5% NaCl solution, *International Journal of Fatigue,* 100 (2017) 285–295.

[8] Perel V.Y., Misak H.E, Mall S., Jain V.K, Biaxial fatigue crack growth behavior in aluminium alloy 5083-H116 under ambient laboratory and saltwater environments, *Journal of Material Engineering Performance,* 24(4) (2015) 1565–72.

[9] Abkenar M.R., Kihl D.P., Manzari M.T., Fatigue tests on aluminium specimens subjected to constant and random amplitude loadings, *ASME Journal of Materials Technology,* 138(2016) 1–7.

[10] Holtz R.L., Pao P.S., Bayles R.A., Longazel T.M., Goswami R., Corrosion fatigue of aluminium alloy 5083-H131 sensitizes at 448 K (175°C), *Metal Materials Transaction A,* 43 A (2012) 2839–2849.

[11] Miller K.W., Chao Y.J., Wang P.C., Performance Comparison of Spot-Welded, Adhesive Bonded, and Self-Piercing Riveted Aluminium Joints, *ASM proceedings of the international conference: trends in welding research,* (1998) 910–915.

[12] Costa J.D.M, Jesus J.S., Loureiro A., Ferreira J.A.M., Borrego L.P., Fatigue life improvement of mig welded aluminum T-joints by friction stir processing, *Internatinal Journal of Fatigue,* 61 (2014) 244–54.

[13] Messler Jr R.W., Principles of welding: processes, physics, chemistry and metallurgy, 1st ed. New York: John Wiley & Sons, (1999).

[14] Ilman M.N., Kusmono, Muslih M.R., Subeki N., Wibowo H., Mitigating distortion and residual stress by static thermal tensioning to improve fatigue crack growth performance of MIG AA5083 welds, *Materials Design,* 99 (2016) 273–283

[15] Mochizuki M., Toyoda M., Weld distortion control during welding process with reverse-side heating, *ASME Journal of Pressure Vessel Technology,* 129 (2007) 619–29.

[16] Han W.T., Wan F.R., Li G., Dong C.L., Tong J.H., Effect of trailing heat sink on residual stresses and welding distortion in friction stir welding Al sheets, *Science Technology Welding Joint,* 16 (5) (2011) 453–8.

[17] Cheng X., Fisher J.W., Prask H.J., Gnaupel-Herold T., Yen B.T., Roy S., Residual stress modification by post-weld treatment and its beneficial effect on fatigue strength of welded structures, *Internatinal Journal of Fatigue,* 25 (2003) 1259–69.

[18] Ipekoglu G., Cam G., Effects of initial temper condition and post weld heat treatment on the properties of dissimilar friction-stir-welded joints between AA7075 and AA6061 aluminium alloys, *Metal Materials Transactions A,* 45 (2014) 3074–87.

[19] Vijay S., Rajanarayanan S., Ganeshan G.N., Analysis on mechanical properties of gas tungsten arc welded dissimilar aluminium alloy (Al2024 & Al6063), *Materials Today: Proceedings,* 21 (2020) 384–391.

[20] Miller, Equipments.Welders. Available at: https://www.millerwelds.com/equipment/welders/mig-gmaw. Retrieved March 2, 2021.

[21] Bunaziv I., Akselsen O.M., Salminen A., Unt A., Fiber laser-MIG hybrid welding of 5 mm 5083 aluminum alloy, *Journal of Materials Processing Technology* ,233 (2016) 107–114.

[22] Yong P., Changbin S., Yadong Z., Ying C., Comparison of Electrochemical Behaviors between FSW and MIG Joints for 6082 Aluminum Alloy, *Rare Metal Materials and Engineering,* 46(2) (2017) 0344-0348.

[23] Schneider C.F., Lisboa C.P., Silva R.A and Lermen R.T., Optimizing the Parameters of TIG-MIG/MAG Hybrid Welding on the Geometry of Bead Welding Using the Taguchi Method, *Journal of Manufacturing and Materials Processing,* (2017) 1- 14.

[24] Subbaiah K., Microstructure and Mechanical properties of Tungsten Inert Gas Welded Joints of Cast Al-Mg-Sc alloy, *Materials Today: Proceedings,* 16 (2019) 248–25.

[25] Zhang C., Baob Y., Zhua H., Niea X., Zhanga W., Zhanga S., Zeng A. A, comparison between laser and TIG welding of selective laser melted AlSi10Mg, *Optics and Laser Technology,* 120 (2019) 105696.

[26] Singh L., Singh R., Singh N. K., Singh D., Singh P,. An Evaluation of TIG Welding Parametric Influence on Tensile Strength of 5083 aluminium Alloy, International Journal of Mechanical, *Industrial Science and Engineering* (2013) 795-798.

[27] Kumar S., Shahi A. S., Effect of heat input on the microstructure and mechanical properties of gas tungsten arc welded AISI 304 stainless steel joints, *Materials and Design,* (2011) 3617–3623.

[28] Jahanzaib M., Hussain S., Wasim A., Aziz H., Mirza A., Ullah S., Modeling of weld bead geometry on HSLA steel using response surface methodology, *The İnternational Journal of Advance Manufacturing Technology,* (2017) 2087 – 2098.

[29] Raveendra A., Kumar B.V.R.R, Sivakumar A., Reddy V.P K., Influence of Welding Parameters on Weld Characteristics of 5052 Aluminium Alloy sheet Using TIG Welding, *International Journal of Application or Innovation in Engineering & Management (IJAIEM),* (2014) 186-190.

[30] Gharibshahiyan E., Raouf A.H., Parvin N., Rahimian M., The effect of microstructure on hardness and toughness of low carbon welded steel using inert gas welding, *Materials & Design,* (2011) 2042–2048.

[31] Liu Y., Wang W., Xiea J., Sunb S., Wang L., Qiana Y., Menga Y., Wei Y., Microstructure and mechanical properties of aluminum 5083 weldments by gas tungsten arc and gas metal arc welding, *Materials Science and Engineering A*, 549 (2012) 7-13.

[32] Hirata T., Oguri T., Hagino H., Tanaka T., Chung S.W., Takigawa Y., Higashi K., Influence of friction stir welding parameters on grain size and formability in 5083 aluminum alloy, *Material Science and Engineering A*, 456 (2007) 344–349.

[33] Peel M., Steuwer A, Preuss M., Withers P.J., Microstructure, mechanical properties and residual stresses as a function of welding speed in aluminium AA5083 friction stir welds, *Acta Materilia*, 51 (2003) 4791–4801.

[34] Haboudou A., Peyre P., Vannes A.B., Peix G., Reduction of porosity content generated during Nd: YAG laser welding of A356 and AA5083 aluminium alloys, *Materials Science and Engineering A*, 363 (2003) 40–52.

[35] James M.N., Hughes D.J., Hattingh D.G., Mills G., Webster P.J., Residual stress and strain in MIG butt welds in 5083-H321 aluminium: As-welded and fatigue cycled, *International Journal of Fatigue*, 31 (2009) 28–40.

[36] Spinelli J.E., Ferreira I.L., Garcia A., Influence of melt convection on the columnar to equiaxed transition and microstructure of downward unsteady-state directionally solidified Sn–Pb alloys, *Journal of Alloys and Compounds*, 384 (2004) 217–226.

[37] Wu C.S., Computer Sımulatıon Of Three-Dımensıonal Convectıon In Travellıng Mıg Weld Pools, *Engineering Computations*, 9 (1992) 529–537.

[38] Mutombo K., Toit M.D., Microstructure and mechanical properties of aluminum 5083 weldments by gas tungsten arc and gas metal arc welding, *Materials Science Forum*, 654–656 (2010) 2560–2563.

[39] Moreira P.M.G.P., Figueiredo M.A.V., Castro P.M.S.T., Fatigue behaviour of FSW and MIG weldments for two aluminium alloys., *Theory Application Fracture Mechanics*, 48 (2007) 169–177.

[40] Kumar K., Mohan P., Masanta M., Influence of welding current on the mechanical property of 3 mm thick commercial 1050 aluminium butt joint weld by AC-TIG welding method, *Materials Today: Proceedings*, 5 (2018) 24141–24146.

[41] Ahmad Ibrahim M. F., Bakar S.R.S., Jalar A., Othman N. K., Sharif J., Daud A. R., Rashdi N. M., Effect of porosity on tensile behavior of welded AA6061-T6 aluminium alloy, *Applied Mechanics and Materials*, (2011) 534-53.

[42] Pessoa E. C. P., Bracarense A. Q., Zica E. M., Liu S., Guerrero F. P., Porosity variation along multipass underwater wet welds and its influence on mechanical properties, *Journal of Materials Processing Technology*, (2006) 239-24.

[43] Borrego L.P., Costa, J.D., Jesus, J.S., Loureiro A.R., Ferreira J.M., Fatigue life improvement by friction stir processing of 5083 aluminium alloy MIG butt welds, *Theoretical and Applied Fracture Mechanics*, 70 (2014) 68-74.

[44] Yürük A., Kaya Y., Kahraman N., Alüminyum Alaşımlarının MIG Kaynak Yöntemi ile Kaynak Edilebilirliğinin İncelenmesi, *Bayburt Üniversitesi Fen Bilimleri Dergisi*, 4(1) (2021).